

# Wigner Crystallization in Two Dimensions: Evolution from Long- to Short-Ranged Forces.

Benjamin M. Fregoso<sup>1</sup> and C. A. R. Sá de Melo<sup>2</sup>

<sup>1</sup>*Joint Quantum Institute and Condensed Matter Theory Center, Department of Physics,  
University of Maryland, College Park, Maryland 20742-4111, USA*

<sup>2</sup>*School of Physics, Georgia Institute of Technology, Atlanta, Georgia 30332, USA*

We study fermions in two dimensions interacting via a long-ranged  $1/r$  potential for small particle separations and a short-ranged  $1/r^3$  potential for larger separations in comparison to a length scale  $\xi$ . We compute the energy of the Wigner crystal and of the homogeneous Fermi liquid phases using a variational approach, and determined the phase diagram as a function of density and  $\xi$  at zero temperature. We discuss the collective modes in the Fermi liquid phase, finite temperature effects on the phase diagram, and possible experimental realizations of this model.

PACS numbers: 71.10.Ca, 71.10.Pm, 05.30.Fk

## I. INTRODUCTION

Inhomogeneity plays an important role in many highly correlated materials<sup>1-8</sup>. For example stripe phases which break translational symmetry of real space in one direction have been observed in high temperature superconductors<sup>4</sup>. Similarly, a Wigner crystal (WC) phase<sup>1</sup> which has only discrete translational symmetry of triangular lattices and six-fold rotational symmetry has been observed in electrons on the surface of liquid helium<sup>2,9</sup> and in ultra-clean two-dimensional hole gases<sup>3</sup>.

For interactions which decay as the power law  $1/r^\alpha$ , a classical argument shows that the potential energy scales with density as  $n^{\alpha/2}$  in two dimensions (2D) and the kinetic energy as  $n$ . The ratio of the potential to the kinetic energy scales as  $n^{\alpha/2-1}$  which becomes  $n^{-1/2}$ , for Coulomb interactions, a constant for  $1/r^2$  and  $n^{1/2}$  for  $1/r^3$  potentials. A stable WC crystal phase occurs when the interaction energy is greater than the kinetic energy<sup>1</sup>. Hence, a WC is expected in the high density regime or low density regime depending on the power law decay of interactions. For Coulomb forces this suggests that there is a phase transition at decreasing densities from a homogeneous Fermi liquid (FL) phase, which is conducting, to a WC phase, which is insulating. In this regime, perturbative methods fail and one must resort to numerical studies<sup>5,6</sup>.

In reality, many important systems do not have pure power law interactions. For two-dimensional electron gases (2DEGs) in semiconductor inversion layers or quantum wells, the presence of a nearby gate modifies the Coulomb interaction. Image charges emerge at the gate and screen the Coulomb ( $1/r$ ) interaction, which become  $1/r^3$  at large distances beyond a length scale given by the distance to the gate. The effects of such long-ranged forces changes the energetics of the 2DEG<sup>10</sup>. Recently, the effects of long-ranged forces on superconductivity have been explored too<sup>11</sup>. A similar experimental scenario occurs in ionic liquid transistors<sup>12,13</sup>, where an electrolyte is used as a dielectric in a standard field effect transistor configuration. Positive and negative charges

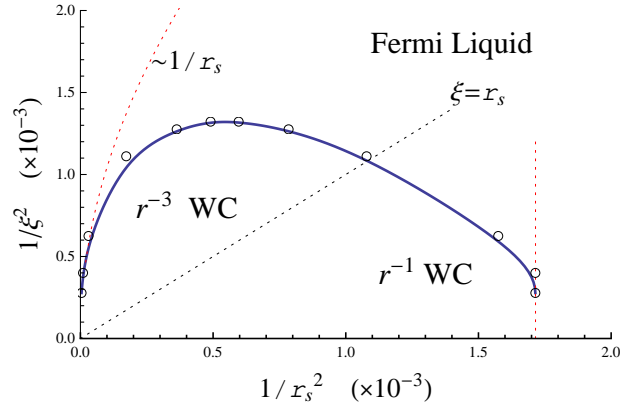


FIG. 1: (Color online) Phase diagram of fermions with two-body interaction Eq. (1). The phase boundary between Wigner crystal (WC) and uniform Fermi liquid (FL) phase as a function of the screening length  $\xi$  in units of  $a_0$  and density  $n = 1/(\pi a_0^2 r_s^2)$ . Circles represent numerical points with 55 electrons and the solid line is a guide to the eye. Also shown is the  $\xi = r_s$  line, which divides the Coulomb  $1/r$  regime (right) from the  $1/r^3$  regime (left).

accumulate at opposite ends of the electrolyte. Finally, recent progress in cooling techniques have allowed the study of degenerate dipolar gases<sup>14-22</sup> including Wigner crystallization of dipoles with  $1/r^3$  potentials<sup>20</sup> and collective modes<sup>21-24</sup>. Such objects interact as  $1/r^3$  at large separations. At short distances the interaction potential is modified by the interactions between the electronic clouds. The common feature of these systems is that there is a length scale in the interactions. They are composed of charges of opposite signs which are located in layers separated by a dielectric. As such, the interparticle potential crosses over between two different power law regimes.

In this work, we study the ground state properties and collective modes of polarized electrons in 2D with screened Coulomb interactions. Such system is realized in 2DEG in the presence of a nearby gate and a magnetic field parallel to the surface to avoid significant orbital ef-

fects. We also describe the related problem of a gas of fermionic dipoles which have a finite size. To be concrete, we consider an interaction interpolating smoothly between a  $1/r$  ( $1/r^3$ ) potential at short (long) distances

$$V(r) = \frac{e^2}{\epsilon r} - \frac{e^2}{\epsilon(r^2 + \xi^2)^{1/2}}, \quad (1)$$

where  $\xi$  represents the screening length. While three dimensional effects have been investigated in a variety of contexts<sup>25</sup>, here, we consider a 2D model. Our phase diagram agrees with studies of 2DEGs with a nearby gate<sup>7,8</sup>, and of electrons on the surface of liquid helium<sup>26</sup>. In our analysis, we consider a many-body wave function in the form of a Slater determinants and variational single-particle wave functions for the FL and WC phases. In the WC phase, the variational parameter is the spatial extent of the single-particle wave functions. Optimizing the total energy at zero temperature we explicitly calculate and compare the ground state energies of the WC and FL phases. We note that the effects of screened interactions on the capacitance of 2DEGs and ionic liquids have also been explored<sup>10,13</sup>.

The corresponding zero-temperature ( $T = 0$ ) phase diagram is presented in Fig. 1 as a function of the length scale  $\xi$  and density  $n$  parametrized by  $r_s = 1/(a_0\sqrt{\pi n})$ , where  $a_0 = \epsilon\hbar^2/(me^2)$  is the Bohr radius in the presence of the dielectric constant  $\epsilon$ . The FL and WC phases are indicated in the phase diagram and are labeled according to the dominant interaction regimes. For fixed  $\xi > \xi_c$  there is a regime of densities where the Wigner crystal is energetically more favorable than a uniform FL. We also show the asymptotic forms of the phase boundaries in dashed (red) lines. In the regime dominated by  $1/r^3$ , the asymptotic phase boundary corresponds to  $\xi \sim r_s^{1/2}$ , while in the Coulomb case it is  $r_s = \text{constant}$  ( $\approx 24.2$ ). Intuitively, for  $1/r^3$  potentials (left of the  $\xi = r_s$  line) the kinetic ( $1/r_s^2$ ) and potential ( $e^2\xi^2/r_s^3$ ) energies are comparable when  $\xi \sim r_s^{1/2}$ , whereas for the  $1/r$  regime, the potential energy scales as  $e^2/r_s$  and these energies are comparable when  $1/r_s^2$  is a constant ( $\approx 1.72 \times 10^{-3}$ ). Notice that for  $\xi < \xi_c = 27.5a_0$  there is no WC phase. The existence of the maximum is a general feature that also follows from the physical argument described above; if  $\xi$  is too small the potential energy cannot be of the same order as the kinetic energy. The limit  $\xi \rightarrow \infty$  (Coulomb regime) is not strictly accessible within our method. However, by extrapolating, we find that the WC phase more favorable than the WC phase for  $r_s > 24.2$ .

For  $\xi < \xi_c$  and increasing density from zero to finite values, we find a first order phase transition from a dipolar FL to a WC. This phase transition has been studied numerically in the context of dipole gases with pure  $1/r^3$  forces<sup>20</sup>. With additional increases of the density beyond the  $\xi = r_s$  line, the WC crosses over to a Coulomb WC. Upon further increase of the density, the WC melts into a FL. This reentrant behavior for the FL phase is a remarkable characteristic of any 2D system interacting

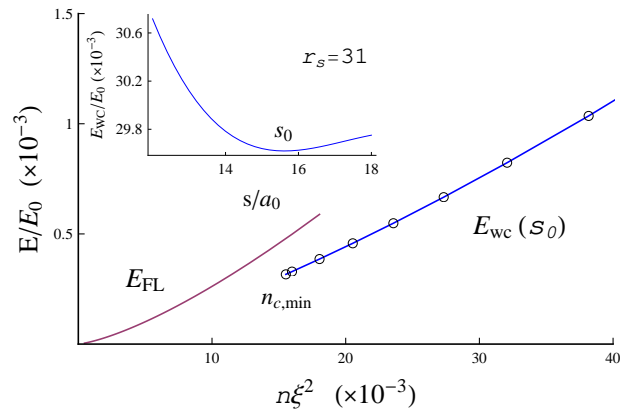


FIG. 2: (Color online) Energy per particle vs density (in units of particles per  $\xi^2$ ) of the WC and FL phases, for  $\xi = 40a_0$ . See also Fig. 3. Inset:  $E_{wc}(s)$  vs size of the wave function.

via an effective potential which crosses over from long to short range. Fig. 1 constitutes one of our main results.

In what follows we show how this phase diagram is obtained. In section II, we present the Hamiltonian and in section III, we compute the energy of the homogeneous FL and discuss its collective modes, as they are modified by the presence of  $\xi$ . In section IV, we obtain the energy in the WC phase with a variational wave function. In section V, we discuss in detail the physical significance of our results, and we compare the energies of these two states in different density regimes in order to determine the ground state of the system. In addition, we discuss the scaling of energy of the WC with respect to density, give a schematic finite temperature phase diagram, and we present our concluding remarks.

## II. MODEL

We start from the microscopic Hamiltonian

$$\hat{H} = - \sum_i \frac{\nabla_i^2}{2m} + \sum_{i < j} V(\mathbf{r}_i - \mathbf{r}_j), \quad (2)$$

where the first term corresponds to the kinetic energy and the second term is given in Eq. (1), which describes the interactions between spinless fermions. The variable  $\xi$  is the ‘screening’ length and we treat it as a phenomenological parameter. It could represent a number of physical quantities, e.g., twice the distance between a polarized 2DEG and a nearby gate or the classical effective size of the dipoles. Here,  $\epsilon$  is the dielectric constant of the medium. Note that for a fixed density and in the limit  $\xi \rightarrow \infty$ , the interaction becomes  $V(r) = e^2/\epsilon r$ . Whereas, in the limit  $\xi \rightarrow 0$ , it becomes  $V(r) = (e\xi)^2/\epsilon r^3$  to lowest non-vanishing order in  $\xi$ . In Section V, we also discuss polarized fermionic dipoles where there is a factor of two in the two-body interaction.

For both FL and WC phases, we consider the many-body ground state wave function to be

$$\Psi(\mathbf{r}_1, \mathbf{r}_2, \dots, \mathbf{r}_N) = \mathcal{A}[\phi_1(\mathbf{r}_1) \cdots \phi_N(\mathbf{r}_N)], \quad (3)$$

where  $N$  is the number of particles, and  $\mathcal{A}$  is an operator that describes the anti-symmetrization necessary for indistinguishable fermions. Results for indistinguishable bosons and for classical distinguishable particles are straight-forward extensions. For simplicity, we assume that the spin degrees of freedom are frozen, such that the wave function describing individual particles  $\phi_\ell(\mathbf{r}_\ell)$  are either plane waves in the FL phase, or Gaussian centered at individual sites of a triangular lattice in the Wigner crystal phase.

### III. FERMI LIQUID PHASE

To begin, let us consider the homogeneous FL phase. Our system has two length scales. The first scale is  $\xi$ , while the second is the interparticle distance  $k_F^{-1}$  set by the density  $n = k_F^2/(4\pi)$ , where  $k_F$  is the Fermi momentum of the FL with Fermi energy  $E_F = k_F^2/2m$ . The relative size of these length scales determines the range of the potential. Using the relation between  $n$ ,  $k_F$  and  $r_s$ , we see that for  $\xi/(a_0 r_s) \ll 1$  the fermions interact with a  $1/r^3$  potential, whereas for  $\xi/(a_0 r_s) \gg 1$  they interact with the Coulomb  $1/r$  potential (see Fig. 1). The energy per particle of a uniform and polarized FL is

$$\begin{aligned} \frac{E_{FL}}{E_0} = & \frac{2}{r_s^2} + \frac{2\bar{\xi}}{r_s^2} - \frac{1}{\bar{\xi}} \left[ I_0(4\bar{\xi}/r_s) - I_2(4\bar{\xi}/r_s) \right. \\ & \left. + \frac{8\bar{\xi}}{\pi r_s} - 1 - L_0(4\bar{\xi}/r_s) + L_2(4\bar{\xi}/r_s) \right], \quad (4) \end{aligned}$$

where  $\bar{\xi} = \xi/a_0$  is scaled by the Bohr radius  $a_0 = \epsilon\hbar^2/me^2$ , and the energy  $E_{FL}$  is scaled by the Bohr energy  $E_0 = e^2/2a_0$ . The functions  $I_n(x)$  are the  $n^{\text{th}}$  order modified Bessel function of the 1st kind and  $L_n(x)$  are the  $n^{\text{th}}$  order Struve functions. In obtaining Eq. (4), we used the fact that the two-body interactions shown in Eq. (1) have Fourier transform  $V(q) = (2\pi e^2/\epsilon q)(1 - e^{-\xi q})$ , where  $q$  is the magnitude of the two dimensional momentum vector.

The first term in Eq. (4) is the kinetic energy and scales as the density  $n$ . The second term in Eq. (4) is the Hartree contribution, which also scales as  $n$ . In the limit  $\bar{\xi} \rightarrow \infty$ ,  $E_{FL}/E_0 = 2/r_s^2 + 2\bar{\xi}/r_s^2 - 16/(3\pi r_s)$  is formally divergent as interaction potential is long-ranged, that is, it behaves as  $1/r$ . In a 2DEG the positive background charge cancels the Hartree term and, in this case,  $E_{FL}/E_0 = 2/r_s^2 - 16/(3\pi r_s)$ , in agreement with known results<sup>27</sup>. The last term within the square brackets is the Fock contribution, which becomes  $-2\bar{\xi}/r_s^2 + 256\bar{\xi}^2/(45\pi r_s^3)$  as  $\bar{\xi} \rightarrow 0$  and leads to  $E_{FL}/E_0 = 2/r_s^2 + 256\bar{\xi}^2/(45\pi r_s^3) + O(\bar{\xi}^3)$  in this  $1/r^3$  regime. To  $O(\bar{\xi})$  the Fock term cancels the Hartree term for pure  $1/r^3$  potentials. Physically, the system behaves as a charge neutral FL of dipoles. We note that including a background

to enforce charge neutrality, as in 2DEGs with  $1/r$  potentials, leads to negative energies and a self-bound system. However, in the present case the energies are positive and the system has positive pressure. The energy of the uniform FL is shown in Fig. 2 for  $\xi = 40a_0$ .

#### A. Collective modes

The length scale  $\xi$  in the potential introduces important modifications to the collective excitations in the FL phase. The Fourier transform of Eq. (1) at zero momentum is well-defined,  $V(0) = 2\pi e^2 \xi$ . For these kinds of forces, it is very important to keep the Hartree and Fock terms in any approximation to the self-energy<sup>28</sup> as this provides a conserving approximation<sup>29</sup>. The collective modes are given by the zeros of the dielectric function  $\epsilon(q, \omega) = 1 - V(q)\Pi(q, \omega)$ . A non-conserving RPA calculation gives,

$$\omega_q = v_F(\bar{\xi}/2)^{1/2} q, \quad (5)$$

for  $\bar{\xi} \gg 1$  and  $\omega_q = v_F[1 + \bar{\xi}^2/2] q$  for  $\bar{\xi} \ll 1$ . Hence, we expect the system to support zero sound modes. A detailed calculation likely renormalizes the zero sound velocity, but does not alter the qualitative physical phenomenon; see, for example, the analysis performed in the context of polarized dipole gases<sup>21–24</sup>. The speed of the zero sound diverges when  $\xi \rightarrow \infty$ , since the power expansion in  $q/\omega_q$  breaks down in this limit. Indeed, the plasmon dispersion relation in 2DEGs has been extensively studied in GaAs<sup>30,31</sup> semiconductor quantum wells. The Fourier transform of the pure Coulomb potential  $V(q) \sim 1/q$  diverges at zero momentum and leads to gapless  $\sim \sqrt{q}$  mode dispersion.

According to the variational principle, the energy obtained using the many-body wave function described in Eq. (3) is a rigorous upper bound for the true ground state energy of the system. In the following analysis, we perform a variational calculation of the ground state energy of the WC phase and compare it with that of the FL phase obtained in Eq. (4).

### IV. WIGNER CRYSTAL PHASE

In the Wigner crystal phase, the single-particle wave functions are localized at sites  $i$  of a 2D triangular lattice,  $\phi_i(\mathbf{r}) = [1/(s\sqrt{\pi})] \exp[-(\mathbf{r} - \mathbf{R}_i)^2/(2s^2)]$ , where  $\mathbf{R}_i$  is the site position and  $s$  parametrizes the 2D size of the wave function. These single-particle wave functions are approximately orthonormal, since the overlap at different sites is exponentially small,  $\int d^2r \phi_i^*(\mathbf{r}) \phi_j(\mathbf{r}) = \exp[-(\mathbf{R}_i - \mathbf{R}_j)^2/4s^2] = \exp[-R_{ij}^2/(4s^2)]$ , provided that the separation  $R_{ij}$  between sites  $i$  and  $j$  is much larger than the extent  $s$  of the single-particle wave function. We denote the lattice spacing by  $l$  and consider the

regime of weakly overlapping single-particle wave functions, where  $s < l/2$ . The localized nature of the many-body wave function is reasonable only in this regime. Explicitly, the energy per particle in the WC phase is,

$$\frac{E_{wc}(\bar{s})}{E_0} = \frac{1}{\bar{s}^2} + \int_0^\infty d\bar{k} (1 - e^{-\bar{\xi}\bar{k}}) e^{-\bar{k}^2 \bar{s}^2/2} F_1(\bar{k}) - \frac{\sqrt{2\pi}}{2\bar{s}} \left( 1 - e^{\bar{\xi}^2/2\bar{s}^2} \text{erfc}\left(\frac{\bar{\xi}}{\sqrt{2\bar{s}}}\right) \right) F_2(\bar{s}), \quad (6)$$

where the functions  $F_i(y)$  are lattice sums given by  $F_1(\bar{k}) = \sum_{i \neq j} J_0(\bar{k}\bar{R}_{ij})/N$  appearing in the second term of Eq. (6), and  $F_2(\bar{s}) = \sum_{i \neq j} e^{-\bar{R}_{ij}^2/2\bar{s}^2}/N$  appearing in the third term of Eq. (6). Here, we defined the dimensionless variables  $\bar{s} = s/a_0$ ,  $\bar{k} = ka_0$ ,  $\bar{R}_{ij} = R_{ij}/a_0$  and  $J_n$  is the  $n^{\text{th}}$  order Bessel function of the first kind. The first term is the zero point motion due to the localization of the particles at the lattice sites. This term favors large single-particle wave functions. The second and third terms are the Hartree-Fock (HF) contribution (respectively). The HF contribution is non-monotonic in  $s$ . The extension to particles with bosonic statistics results in a change of the sign of the Fock term whereas for classical particles only the Hartree term is present.

We comment on the limiting behavior of Eq. (6). Fermions interact via a Coulomb potential when  $\xi \rightarrow \infty$ . In this limit, the ground state energy is

$$\frac{E_{wc}^{\text{Coulomb}}}{E_0} = \frac{1}{\bar{s}^2} + \frac{\sqrt{2\pi}}{2\bar{s}N} \sum_{i \neq j} e^{-\bar{R}_{ij}^2/4\bar{s}^2} I_0(\bar{R}_{ij}^2/4\bar{s}^2) - \frac{\sqrt{2\pi}}{2\bar{s}N} \sum_{i \neq j} e^{-\bar{R}_{ij}^2/2\bar{s}^2}. \quad (7)$$

In the regime of non-overlapping wave functions  $l/2s \gg 1$ , the asymptotic form of the Bessel function is  $I_0(x) \sim e^x/\sqrt{2\pi x}$ . As we see, the series in the second (Hartree) term diverges when  $N \rightarrow \infty$  as expected, since we have not included a neutralizing background charge. In this case, taking a finite  $N$  gives a well defined energy which is non-monotonic in  $s$ . We find that this behavior extends to the regime of  $\xi < \infty$  and produces a WC state energy  $E_{wc}(s)$  that does not have a minimum as a function of  $s$ , when the density is either too small or too large. On the other hand, in the limit of  $\xi \rightarrow 0$ , we obtain that the  $O(\xi)$  contribution from the Fock term cancels the Hartree term (as in the FL phase) and the first non-vanishing term is  $O(\xi^2)$ . Since the resulting expression is not very illuminating, we omit it here.

## V. DISCUSSION AND CONCLUSIONS

For  $\xi < \infty$ , the integral appearing in Eq. (6) needs to be calculated numerically. We computed the energy per particle as a function of density  $n = 2/(l^2\sqrt{3})$  in the WC phase for a 2D triangular array of 43 and 55 particles.

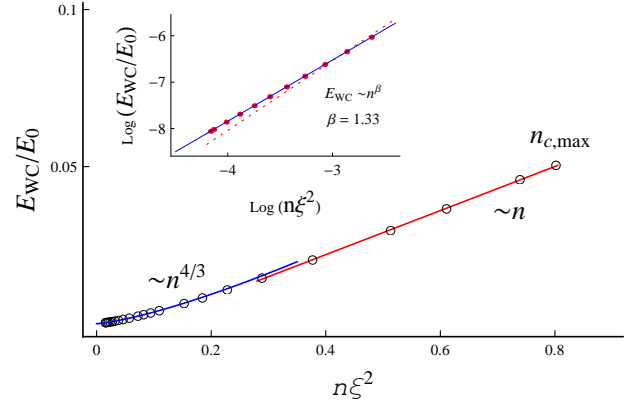


FIG. 3: (Color online) Scaling of the energy  $E_{wc}$  of the Wigner crystal (WC) near  $n_{c,min}$  and  $n_{c,max}$ . Here,  $\xi = 40a_0$ . The picture shows two different scalings with density. The crossover occurs at  $r_s = \xi/a_0$  where  $n\xi^2 = 1/\pi$ . Inset shows a fit at low densities (blue line) and the classical  $\sim n^{3/2}$  scaling of the WC (red-dashed line).

In Fig. 1, we show the resulting phase diagram for 55 particles, but we would like to emphasize that the qualitative behavior found is essentially unchanged for higher number of particles. The calculation of phase boundaries for the full range of parameters  $\xi$  and  $r_s$  is very intensive when it involves a large number of particles, however, we do not expect any major qualitative changes in behavior.

We establish the phase boundary between solid and liquid phases by minimizing the energy in the solid phase with respect to the variational parameter  $s$ . A typical behavior of the energy as a function  $s$  is shown in Fig. 2. When there is a local minimum of  $E_{wc}(s)$  located at  $s = s_0$ , we compare the energy  $E_{wc}(s_0)$  with the energy of the screened FL with the same density. We find that the energy of the WC is always lower than the FL energy in the regime of tested values of  $\xi$ . However, a local minimum of  $E_{wc}(s)$  does not exist for densities below a minimum  $n_{c,min}(\xi)$  and for densities above a maximum  $n_{c,max}(\xi)$ , where the WC phase is unstable. This establishes that the WC phase is unstable for densities  $n$  satisfying the condition  $n < n_{c,min}(\xi)$  and  $n > n_{c,max}(\xi)$ , in which case, the FL phase is the stable phase.

A phase transition from a ferromagnetic FL to a ferromagnetic WC phase in a 2DEG with  $1/r$  interactions is expected to occur at  $r_s = 29$  according to recent Monte-Carlo simulations<sup>6</sup>. In the  $\xi \rightarrow \infty$  limit, we find such a phase transition at  $r_s = 24.2$ , with finite-sized samples. We note that our results do not rigorously apply in this regime since interactions are of pure Coulomb character and a neutralizing background charge must be explicitly considered. Here, we are interested in the regime of  $\xi < \infty$ , where our results are expected to be qualitatively correct.

We note that the optimized energy values in the WC can be fitted with a power law

$$E_{wc}(s_0) \sim n^{4/3} \quad (8)$$



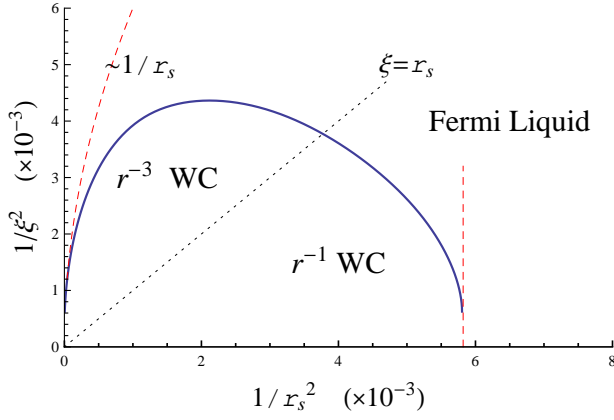


FIG. 4: (Color online) Phase diagram of dipoles with effective size  $\xi$  in 2D, versus density ( $1/r_s^2$ ). The Fermi liquid (FL) and Wigner Crystal (WC) phases are indicated.

in the low density regime, i.e.,  $r_s \gg \xi$  where interactions are of  $1/r^3$  character. This is shown explicitly in Fig. 3 for  $\xi = 40a_0$ . We tested the scaling for  $40 < \xi/a_0 < 60$  to within 1% error, but we cannot completely rule out a crossover behavior<sup>32</sup>. A similar  $n^{4/3}$  scaling behavior has been studied in 2DEGs with a  $1/r^3$  potential and spin-orbit interactions<sup>33</sup>. In the high density regime ( $r_s \ll \xi$ ) the energy is a linear power law of the density  $E_{wc} = A|n - n_{c,max}| + B$ , where interaction are of  $1/r$  character. This scaling persists in the same tested range and within the same error.

As mentioned earlier, the potential shown in Equation Eq. (1) describes the interactions between polarized electrons in a clean 2DEG with a nearby gate. As is well known, by applying a magnetic field parallel to the surface one avoids significant orbital effects and a one component 2DEG is obtained. However, disorder is always present and makes it difficult to reach the low density regime where the reentrant FL is predicted.

In contrast, another system where disorder does not play a role, corresponds to degenerate polarized dipolar Fermi gases<sup>14,15</sup>. We extended our results to describe a system of dipoles in 2D whose centers move in the plane perpendicular to the polarization axis<sup>34</sup>. In this case,  $\xi$  could parametrize a hard core radius (or size of the molecule) below which interactions are no longer of the  $1/r^3$ . In this new situation, the interaction potential of Eq. (1) acquires a prefactor of two, but the calculations are entirely analogous. In Fig. 4 we show the phase diagram for 43 dipoles. We observe the same features as for screened 2DEGs. For  $\xi < \xi_c = 15a_0$  there is no stable WC phase. In the Coulomb limit the WC is stable for  $r_s > 13a_0$ . In the expressions for the energy of the FL and WC a prefactor of 2 is needed in the interaction energy. The collective modes dispersion is  $\omega_q = v_F \bar{\xi}^{1/2} q$  for  $\bar{\xi} \gg 1$  and  $\omega_q = v_F [1 + 2\bar{\xi}^2] q$  for  $\bar{\xi} \ll 1$ . Our results suggest that realistic dipole gases with size  $\sim 10a_0$ , are Fermi liquids at low *and* very high densities. We provided estimates for the critical densities as a function

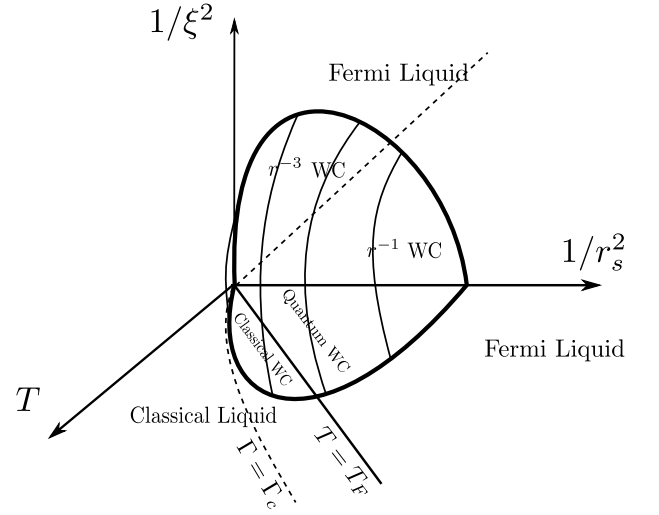


FIG. 5: Schematic phase diagram as function of density  $\sim 1/r_s^2$ , temperature  $T$  and screening parameter  $\xi$  in appropriate units.  $\Gamma$  is the ratio of the potential to kinetic energy. See text for details.

of  $\xi$  in a simplified model. If only  $1/r^3$  interactions are considered<sup>20</sup> one expects a WC instability with increasing densities near the dashed red line on the left in Fig. 4, where the interaction energy is of the order of the kinetic energy. However this red dashed line is strongly modified (blue line), when the hard core is considered.

### A. Finite temperature phase diagram

Next, we discuss the finite temperature phase diagram of the 2DEG with screened interactions. The assumption is that the interactions can be modeled with the simple form Eq. (1). At finite temperatures, we expect the melting of the WC to a liquid-like state<sup>35</sup>. In Fig. 5, we show the phase diagram in the  $(T, n, 1/\xi^2)$  parameter space. In the  $1/\xi^2 = 0$  plane, the thermodynamics of the classical 2DEG is determined by the quantity  $\Gamma$ , which is the ratio of the interaction energy to the kinetic energy per particle. For a classical 2DEG, this ratio is  $\Gamma = (\pi n)^{1/2} e^2 / T$ . For  $\Gamma < 1$ , the kinetic energy dominates and the system behaves as a classical liquid. For  $\Gamma \gg 1$ , the Coulomb interaction dominates and we expect a classical WC. The phase boundary is given by the criterion<sup>2</sup>  $\Gamma = \Gamma_c \sim 100$ . For temperatures below  $E_F \sim n \sim 1/r_s^2$ , we obtain a quantum WC. At high densities the melting temperature is eventually driven down with increasing density as the Pauli principle prevents strong correlations. There is a quantum phase transition in the regime with pure Coulomb interactions at  $r_s \approx 24.2$ . This transition can be seen along the  $1/r_s^2$  line in Fig. 5, where  $\Gamma \sim n^{-1/2}$  in the Hartree-Fock approximation. This defines a critical density above which  $\Gamma < 1$  and a quantum fluid is recovered. The full melting line and the quantum/classical crossover

in the plane  $1/\xi^2 = 0$  is sketched in Fig. 5, see also<sup>31</sup>. Connecting the WC phases of the  $1/\xi^2 = 0$  and  $T = 0$  planes is a dome, where a WC is stable. Within this dome there exists at least four regions corresponding to quantum vs classical and  $1/r$  vs  $1/r^3$  regimes. Outside the dome there are only quantum and classical liquid-like phases.

In conclusion, we have obtained the phase diagram of fermions with interactions which interpolate smoothly between short-ranged and long-ranged regimes in 2D. The phase diagram obtained is generic to any system

with such crossover, e.g, clean 2DEGs in semiconductor inversion layers or quantum wells in the presence of a screening gate, and polarized dipolar gases.

### Acknowledgments

We thank V. Yakovenko for helpful discussions and the JQI-PFC (BMF) and ARO (W911NF-09-1-0220) (CSdM) for support.

- 
- <sup>1</sup> E. Wigner, Phys. Rev. **46**, 1002 (1934).
  - <sup>2</sup> C. C. Grimes and G. Adams, Phys. Rev. Lett. **42**, 795 (1979).
  - <sup>3</sup> J. Yoon, C. C. Li, D. Shahar, D. C. Tsui, and M. Shayegan, Phys. Rev. Lett. **82**, 1744 (1999).
  - <sup>4</sup> S. A. Kivelson, I. P. Bindloss, E. Fradkin, V. Oganessian, J. M. Tranquada, A. Kapitulnik, and C. Howald, Rev. Mod. Phys. **75**, 1201 (2003).
  - <sup>5</sup> B. Tanatar and D. M. Ceperley, Phys. Rev. B **39**, 5005 (1989).
  - <sup>6</sup> N. D. Drummond and R. J. Needs, Phys. Rev. Lett. **102**, 126402 (2009).
  - <sup>7</sup> B. Spivak, Phys. Rev. B **67**, 125205 (2003).
  - <sup>8</sup> B. Spivak and S. A. Kivelson, Phys. Rev. B **70**, 155114 (2004).
  - <sup>9</sup> E. Rousseau, D. Ponarin, L. Hristakos, O. Avenel, E. Varoquaux, and Y. Mukharsky, Phys. Rev. B **79**, 045406 (2009).
  - <sup>10</sup> B. Skinner and M. M. Fogler, Phys. Rev. B **82**, 201306(R) (2010).
  - <sup>11</sup> S. Raghu, E. Berg, A. V. Chubukov, and S. A. Kivelson, arXiv:1111.2982v1.
  - <sup>12</sup> J. H. Cho, J. Lee, Y. Xia, B. Kim, Y. He, M. J. Renn, T. P. Lodge, and C. D. Frisbie, Nature Materials **7**, 900 (2008).
  - <sup>13</sup> M. S. Loth, B. Skinner, and B. I. Shklovskii, Phys. Rev. E **82**, 056102 (2010).
  - <sup>14</sup> M. Lu, N. Q. Burdick, and B. L. Lev, Phys. Rev. Lett. **108**, 215301 (2012).
  - <sup>15</sup> K.-K. Ni, S. Oospelkaus, M. H. G. de Miranda, A. Pe'er, B. Neyenhuis, J. J. Zirbel, S. Kotochigova, P. S. Julienne, D. S. Jin, and J. Ye, Science **322**, 231 (2008).
  - <sup>16</sup> M. A. Baranov, M. Dalmonte, G. Pupillo, and P. Zoller, Chem. Rev. **112** (9), 50125061 (2012).
  - <sup>17</sup> K. Maeda, T. Hatsuda, and G. Baym, Phys. Rev. A **87**, 021604(R) (2013).
  - <sup>18</sup> K. Sun, C. Wu, and S. Das Sarma, Physical Review B **82**, 075105 (2010).
  - <sup>19</sup> C. Lin, E. Zhao, and W. V. Liu, Phys. Rev. B **81**, 045115 (2010).
  - <sup>20</sup> N. Matveeva and S. Giorgini, Phys. Rev. Lett. **109**, 200401 (2012).
  - <sup>21</sup> M. Babadi and E. Demler, Phys. Rev. A **86**, 063638 (2012).
  - <sup>22</sup> M. Babadi and E. Demler, Phys. Rev. A **84**, 033636 (2011).
  - <sup>23</sup> Z.-K. Lu and G. V. Shlyapnikov, Phys. Rev. A **85**, 023614 (2012).
  - <sup>24</sup> J. P. Kestner and S. DasSarma, Phys. Rev. A **82**, 033608 (2010).
  - <sup>25</sup> G. Rastelli, P. Quémerais, and S. Fratini, Phys. Rev. B **73**, 155103 (2006).
  - <sup>26</sup> F. M. Peeters and P. M. Platzman, Phys. Rev. Lett. **50**, 2021 (1983).
  - <sup>27</sup> A. K. Rajagopal and J. Kimball, Phys. Rev. B **15**, 2019 (1977).
  - <sup>28</sup> B. M. Fregoso and E. Fradkin, Phys. Rev. B **81**, 214443 (2010).
  - <sup>29</sup> L. P. Kadanoff and G. Baym, *Quantum Statistical Mechanics* (Benjamin, New York, 1962).
  - <sup>30</sup> M. Eriksson, A. Pinczuk, B. Dennis, C. Hirjibehedin, S. Simon, L. Pfeiffer, and K. West, Physica E **6**, 165 (2000).
  - <sup>31</sup> E. H. Hwang and S. DasSarma, Phys. Rev. B **75**, 205418 (2007).
  - <sup>32</sup> E. H. Lieb and R. Seiringer, J. P. Solovej, Phys. Rev. A **71**, 053605 (2005).
  - <sup>33</sup> E. Berg, M. S. Rudner, and S. A. Kivelson, Phys. Rev. B **85**, 035116 (2012).
  - <sup>34</sup> K. Mitra, C. J. Williams, and C. A. R. Sá de Melo, arXiv:0903.4655 [cond-mat.other].
  - <sup>35</sup> D. R. Nelson and B. I. Halperin, Phys. Rev. B **19**, 2457 (1979).